ISSN 1840-4855
e-ISSN 2233-0046

Review article
http://dx.doi.org/10.70102/afts.2025.1833.100

A COMPARATIVE STUDY OF ADVANCED CONTROL STRATEGIES FOR INTERLINK CONVERTERS IN HYBRID RENEWABLE ENERGY MICROGRIDS

P. Sai Sampath Kumar[1*], P. Suresh[2], D. Lenine[3]

[1]Department of Electrical and Electronics Engineering, SRM Institute of Science and Technology, Kattankulathur, Chennai, Tamilnadu, India; Department of Electrical and Electronics Engineering, RGM College of Engineering &Technology, Nandyal, India. e-mail: sammitsme@gmail.com, orcid: https://orcid.org/0000-0001-9015-8319
[2]Department of Electrical and Electronics Engineering, SRM Institute of Science and Technology, Kattankulathur, Chennai, Tamil Nadu, India. e-mail: suresh.au95@gmail.com, orcid: https://orcid.org/0000-0001-6251-8102
[3]Department of Electrical and Electronics Engineering, RGM College of Engineering &Technology, Nandyal, Andhra Pradesh, India. e-mail: lenine.eee@gmail.com, orcid: https://orcid.org/0000-0001-8816-1631

Received: April 12, 2025; Revised: July 21, 2025; Accepted: August 14, 2025; Published: September 12, 2025

ABSTRACT

This paper derives a novel direct model predictive based power controller (DMPPC) for renewable energy systems (RES) to address voltage fluctuations caused by varying power demands and renewable source outputs. This method utilizes the bi-directional DC-DC converter in the Battery Energy Storage (BES) System to level the renewable energy output, also maintain DC bus voltage stability, with the assistance of fuzzy decision making. Based upon grid necessities and the BES system's state of charge, the controller controls an AC/DC interlinking converter to ensure consistent AC potential and appropriate power exchange with the utility grid. This paper presents an enhanced model predictive controller with an objective function based on fuzzy objectives and limitations that dynamically adapts to external circumstances, instead of utilizing a layered control structural design for BES planning and grid control. With the aid of simulation models created with Matlab Simulink, the suggested controller's operability is confirmed. This approach demonstrates excellent reference tracking performance with minimal Total Harmonic Distortion (THD) with both non-linear as well as linear loads. This article presents the development of a basic hybrid microgrid prototype.

Key words: *renewable energy systems, direct model predictive based power controller, battery energy systems, fuzzy, total harmonic distortion*

INTRODUCTION

Interest in renewable energy source (RES) based generation technologies, like grid-connected solar and wind turbines, has increased recently [10]. Grid-connected inverters are essential components of distributed energy systems [13]. Therefore, inverter control is crucial in ensuring the effective operation of grid-tied inverter systems. Integrating technical innovations with financial strategies can enhance power generation through a hybrid system [8][30]. The system incorporates a diverse range of renewable

energy sources alongside storage solutions. Hybrid wind, solar and battery systems are showing their appeal and affordability for both off-grid and utility-connected applications.[1][2].

Hybrid AC/DC microgrids have recently seen a surge in interest due to the growing deployment of DC sources, alongside concerns about the aging AC power infrastructure that has been in place for over a century. These kinds of microgrids typically use cascading inner current as well as outer voltage loop connections with PID controllers to regulate DC to DC converters as well as AC/DC interlinking circuits [3]. Modifications to the AC-DC switching circuit ensure a consistent frequency and voltage during island mode of the AC sub-grid, while a bidirectional DC-DC converter serves as a voltage regulator for the DC link. Both the utility and the microgrid exchange power with a constant DC-link voltage in grid-operated mode, facilitated by the AC-DC interlinking converter [4][23].

Within the hybrid PV/wind/battery production system, the primary causes of electrical power quality issues are harmonic generation, voltage fluctuations, and frequency fluctuations. In fact, non-linear components such as power converters and loads are the primary causes of harmonics. In addition, changes in methodical issues conditions and network disturbances are the main causes of fluctuations in voltage and frequency [5][31]. Creating the right control regulations over power converters within hybrid systems is one method to solve these concerns.

While utilized as spinning reserve, storage systems are primarily added to mix of energy in order to address such stability concerns. They store energy produced by wind and solar power plants during off-peak hours and assist in voltage as well as frequency adjustment at the point of common coupling (PCC). In addition, energy storage is employed to reduce peak load and enable black-start. Since battery energy storage systems (BESS) can quickly adjust to offset the dynamic discrepancies in electricity production and consumption, they have shown to be a practical solution in dealing with such challenges [27][28]. Fleets of combined electric vehicles (EVs) have the capacity to function as BESSs as well.

Complex control techniques can now be implemented thanks to advancements in processing power. One such promising control method is model predictive control (MPC), which can be used with systems that have accurate mathematical models [9],[29][7][17]. A linear mathematical model can simulate the functioning of a typical VSC, making MPC control a more appropriate option. On the other hand, human knowledge is used to define control objectives and commands in fuzzy control established on fuzzy based decision making (FDM), which eliminates the need for a mathematical model. Because of large parameter variations and a dearth of necessary data, the majority of real-life circumstances are difficult to mathematically model and instead relying on estimates or generalizations [25]. FLC necessitates a solid qualitative grasp of the plant, and the controller's goal is to mimic human thought processes and reasoning. Recent advances in artificial intelligence-based evolving rules and data clustering have made it possible to derive fuzzy inference [11][14][12].

A fuzzy based gain scheduling pattern to the PID controller is presented in [15] in order to enhance the PV farm's transient performance. Fuzzy-MPC control applies to complex and dynamic control systems by combining traditional MPC and FDM [16][18]. Fuzzy based MPC controllers could be utilized to design the objective functions of MPC with multiple conditions FDM or for systems with non-linear models [19]. A fuzzy logic modelled duty cycle modulation procedure for enhanced (MPDPC) is proposed by the authors of [20][21]. Certain systems necessitate distinct control over the elements of the function in order for the extent of influence to fluctuate dynamically in response to experience-backed human knowledge.

In this paper mainly the concept of FDM based predictive control for grid-connected converter control and the examination of its applicability in automatically controlling the converter to regulate a BESS's bidirectional power flow in accordance with dynamic system conditions is established [22][24]. In the MATLAB Simulink environment, a fuzzy-DMPPC structure is proposed and its performance is analytically demonstrated [26][6]. Section II discusses the proposed circuit and its switching states. DMPPC for the specific system is developed and its integration with fuzzy is briefed in section III. Section IV illustrates the outcomes of the simulation, while Section V provides a summary of the findings.

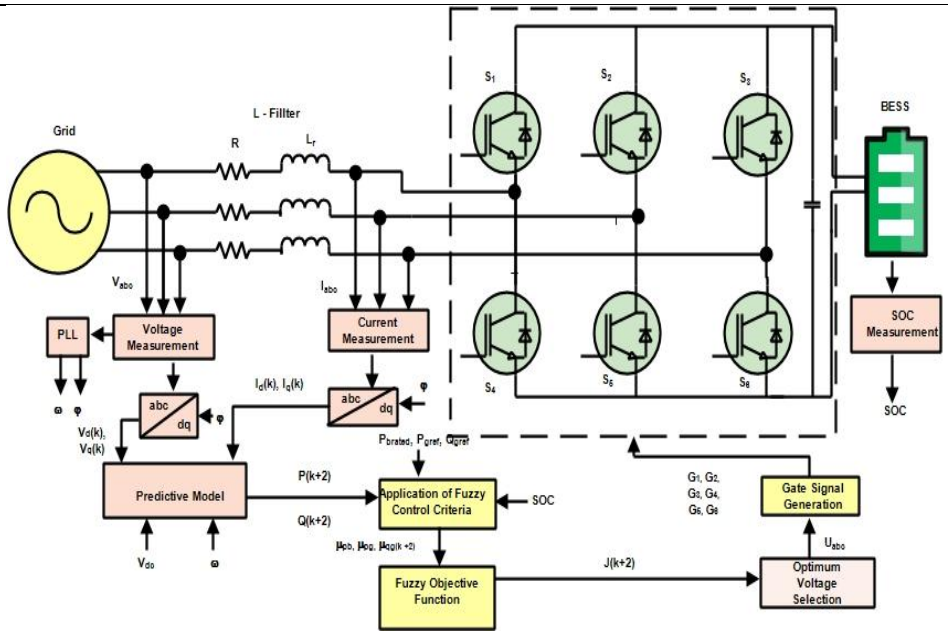

Figure 1. Circuit Schematic of the Proposed Design

CONFIGURATION OF THE CIRCUIT PROPOSED

One type of multilevel inverter that is frequently used in various applications is the 3-φ, Diode clamped three level inverter. The block diagram of the proposed topology is shown in Figure 1, which utilizes a twelve-device switching circuit employing six clamping diodes (Figure 2). These components are combined to create twelve distinct active voltage vectors by configuring the switching states in various ways. The sector is identified using a three-phase reference voltage to generate the gating signals necessary for operating the inverter. Subsequently, the appropriate vector voltages are selected from the table of switching states.

The SVMT method refers to digital modulating procedure that generates PWM according to the vector illustration. These digital signals are delivered straight to switches that are vector representation-managed. The vectors have been organized in the shape of a hexagon to represent the phases and magnitudes of every vector. The SVMT, which is denoted by the α-β axis, is the conventional approach. Three phase voltages that are balanced can be represented by two phase voltages. The coordinate transformation of d-q out of a-b-c can be produced using equations (1) and (2) that follow.

$$V_q = \frac{2}{3}\left(V_a - \frac{1}{2}(V_b + V_c)\right) \quad (1)$$

$$V_d = \frac{1}{\sqrt{3}}(V_b - V_c) \quad (2)$$

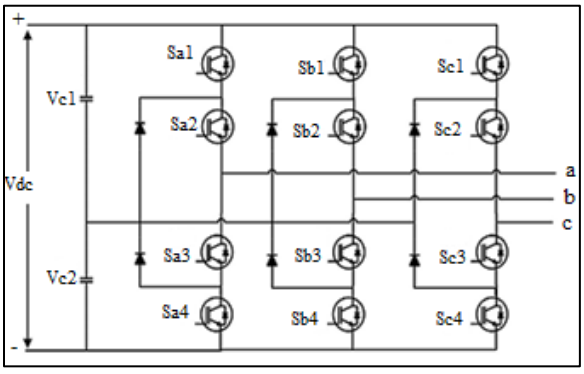

Figure 2. Circuit Configuration Proposed

Using the line voltage as a reference, Equations (3) and (4) facilitate the transformation of RMS voltage from three-phase to d-q (two-phase) parameters.

$$V_{iq} = \sqrt{\frac{3}{2}}\, V_q \quad (3)$$

$$V_{id} = \sqrt{\frac{3}{2}}\, V_d \quad (4)$$

$$\theta = \tan^{-1}\left(\frac{V_{id}}{V_{iq}}\right) \quad (5)$$

The reference voltage's angular position can be evaluated through Equation (5). An inverter consisting of three levels divides each cycle into 27 sectors. The switching table is constructed using the divided sector, the associated potential vector, and the switching state. For example, in sector 2 reference voltage picks the vector voltage V2. The associated switching pattern is represented as (0-1-0-1-0-1). In this work, the conventional α-β approach is applied. The axes of β and α are respectively positioned along 0° and 90°. The reference voltage is provided by the following equation (6). Table 1 provides a summary of the different states. Here CMV indicates the Common Mode Voltage VCMV= (Vao+ Vbo + Vco)/3

$$V_{ref} = \frac{2}{3}\,(V_a + \alpha V_b + \alpha^2 V_c) \quad (6)$$

Table 1. Representation of Various Switching States

Sector	Voltage vector	CMV	State of Switches					
			Sa1	Sa2	Sb1	Sb2	Sc1	Sc2
1	V1	Vdc/2	1	1	1	1	1	1
2	V2	0	0	1	0	1	0	1
3	V3	-Vdc/2	0	0	0	0	0	0
4	V4	Vdc/6	1	1	0	1	0	1
5	V5	Vdc/6	0	1	0	1	1	1
6	V6	Vdc/6	0	1	1	1	0	1
7	V7	Vdc/3	1	1	1	1	0	1
8	V8	Vdc/3	1	1	0	1	1	1
9	V9	Vdc/3	0	1	1	1	1	1
10	V10	-Vdc/3	0	1	0	0	0	0
11	V11	-Vdc/3	0	0	0	0	0	1
12	V12	-Vdc/3	0	0	0	1	0	0
13	V13	-Vdc/6	0	1	0	1	0	0
14	V14	-Vdc/6	0	1	0	0	0	1
15	V15	-Vdc/2	0	0	0	1	0	1
16	V16	0	1	1	0	1	0	0
17	V17	0	0	1	1	1	0	0
18	V18	0	0	0	1	1	0	1
19	V19	0	0	0	0	1	1	1
20	V20	0	0	1	0	0	1	1
21	V21	0	1	1	0	0	0	1
22	V22	Vdc/6	1	1	1	1	0	0
23	V23	Vdc/6	0	0	1	1	1	1
24	V24	Vdc/6	1	1	0	0	1	1
25	V25	-Vdc/6	1	1	0	0	0	0
26	V26	-Vdc/6	0	0	1	1	0	0
27	V27	-Vdc/6	0	0	0	0	1	1

PROPOSED CONTROLLERS DESIGN

(A) DMPPC Control Algorithm

To address control challenges, the voltage expressions of the network are transformed into the voltage-oriented dq reference frame using power-invariant dq transformation. This transformation yields the dq components of the voltage at the grid side, the voltage at the converter side, and the current on the grid side within the voltage-oriented dq reference frame, denoted as Udq, Vdq, and idq, respectively.

$$U_{dq} = V_{dq} + R \cdot i_{dq} + L_f \cdot \frac{di_{dq}}{dt} \quad (7)$$

To use MPC digitally, the system expression (7) needs to be in the discrete domain. Consequently, the forward Euler transformation is utilized to convert differential equations into difference equations. The system's discrete state space form is provided in (8).

$$x(k+1) = A \cdot x(k) + B \cdot u(k) + M \quad (8)$$

In the above equation the state variable x is given by equation (9) and other parameters are represented by the equations (10) to (13) that follows,

$$x = \left[i_d , i_q\right]^T \quad (9)$$

$u = \left[V_d , V_q\right]^T$ represents the input (10)

$$A = \begin{bmatrix} \left(1 - \frac{T_s R}{L_f}\right) & T_s\omega \\ -T_s\omega & \left(1 - \frac{T_s R}{L_f}\right) \end{bmatrix} \text{ represents State Matrix} \quad (11)$$

$$\text{input Matrix } B = \left[-\frac{1}{L_f} , -\frac{1}{L_f}\right] \quad (12)$$

$$M = \left[\frac{U_d}{L_f} , \frac{U_q}{L_f}\right] \quad (13)$$

The instantaneous power theory states that expression (14) can be used to calculate the real power & reactive power of the $(k+2)^{th}$ position at PCC.

$$\begin{bmatrix} P(k+2) \\ Q(k+2) \end{bmatrix} = \begin{bmatrix} \left(1 - \frac{T_s R}{L_f}\right) & T_s\omega \\ -T_s\omega & \left(1 - \frac{T_s R}{L_f}\right) \end{bmatrix} \begin{bmatrix} P(k+1) \\ Q(k+1) \end{bmatrix} + \frac{T_s}{L_f} \begin{bmatrix} U_d\,(k+2) \cdot\ V_d(k+1) - V_d^2\,(k+1) \\ -U_q\,(k+2) \cdot\ V_q(k+1) \end{bmatrix} \quad (14)$$

The expression (6) is used to predict the reactive as well as active power values for the 27 converter voltage vectors previously mentioned in table 1. The switching condition associated with the vector voltages that yields the lowest cost of a predetermined objective function is then applied to the converter in the subsequent control cycle.

(B) Fuzzy Control Algorithm

Fuzzy control is significant because it uses a set of rules to integrate concepts from human understanding into control rules. Usually, a system-experienced operator or design engineer specifies this set of guidelines. The fuzzy-DPMPC defined control criteria are as follows. In order to extend the life of costly BESS and to maximize its benefits, proper control of power is necessary. As a result, a minimal SOC threshold λ1 is established for battery discharge. When the SOC level reaches λ2, the battery begins to charge, and reactive power can be released until the state of charge reaches λ1. When the battery reaches

a SOC level of λ3, it can be used freely for grid conditions.

We define the error functions as equation (15-17). The error costs for real, reactive, & battery power are denoted by the letters ep, eq, and eb in this case. Additionally, as provided in equation (18), the functions μpg, μqg, and μpb, represent the degrees of membership and are defined as exponential expressions. The normalization factors Kp, Kq, and Kb are used to scale μ based on the errors in real power, reactive power, and battery power. While the error is small, the exponential model is selected to enhance its influence on the objective function. The design engineer should define all of these ambiguous criteria along with the settings of parameters in accordance with the specifications and performance needs of the system. The design criteria for membership functions are met, and the appropriate SOC range to govern BESS's operation is established according this article as presented in figure 3. It shows in Figure 4 the fundamental proposed block diagram of fuzzy based MPC control structure.

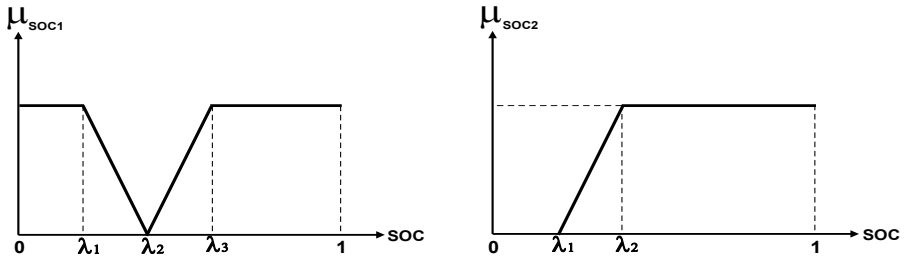

Figure 3. Active & Reactive powers SOC Conditions

$$Er_p(\mathrm{k}+2) = \mathrm{P}(\mathrm{k}+2) - (P_{g_{ref}} \cdot \gamma_{SOC1}) \quad (15)$$

$$Er_q(\mathrm{k}+2) = \mathrm{Q}(\mathrm{k}+2) - (Q_{g_{ref}} \cdot \gamma_{SOC2}) \quad (16)$$

$$Er_b(\mathrm{k}+2) = \mathrm{P}(\mathrm{k}+2) - (P_{b\_rat} \cdot \gamma_{SOC1}) \quad (17)$$

$$\mu_{p_g,q_g,p_b} = \begin{cases} exp\left(\frac{e_{p,q,b}\,(k+2)}{K_{p,q,b}}\right) & -\infty < e(k+2) < 0 \\ exp\left(-\frac{e_{p,q,b}\,(k+2)}{K_{p,q,b}}\right) & 0 \le e(k+2) < \infty \end{cases} \quad (18)$$

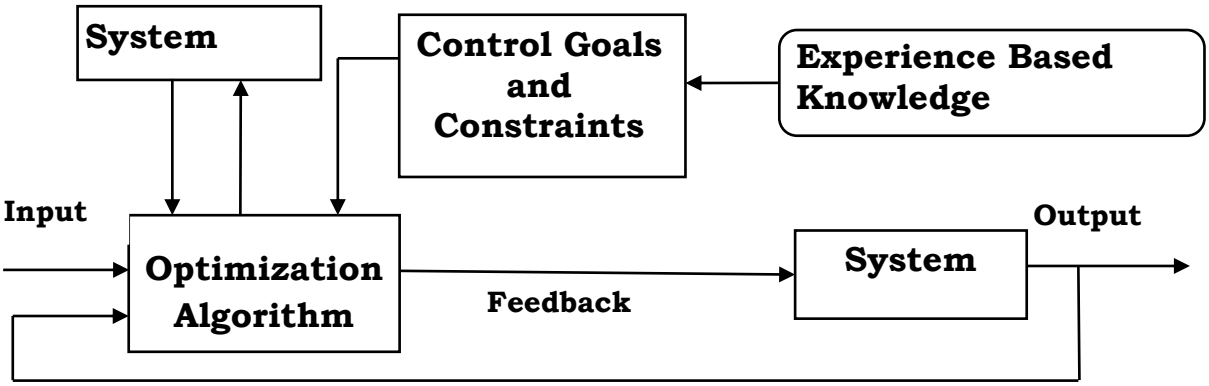

Figure 4. Basic Structure of the Proposed FLC Based MPC

HARDWARE AND SIMULATION RESULT COMPARISON

The proposed SMC and MPV controller for the proposed configuration has been modelled and simulated using MATLAB/Simulink. The findings of the analysis are presented. For simulation, a solar PV system with 12 modules, each with a voltage of 64.2 V, a power of 305 W, and a current rating of 5.96 A is taken into consideration. Figure 5 shows the prototype model for the proposed system.

Figure 5. Hardware Photograph of Proposed System

For the simulation, the wind energy system is configured with the following specifications: voltage = 250 V, power output = 500 W and wind speed = 11 m/s². Table 2 outlines the parameters used in the simulation.

Table 2. System Configuration Parameters

Parameter	**Value**
Voltage across the DC link	V_{dc}= 220 Volts
Capacitor Filter	C =100 µF
Inductance Filter	L =0.09 H
Sampling time	Ts =20 µsec
A Resistive load, R	30 Ohms
The Value of PI techniques Kp& Ki	27& 3

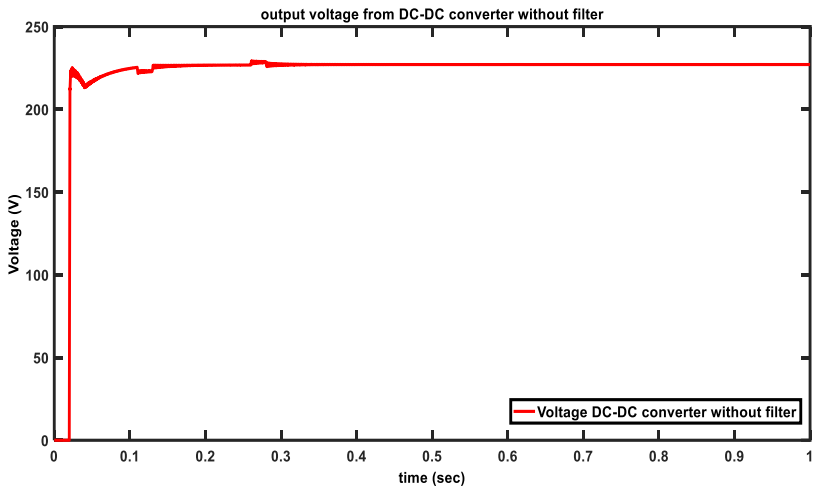

Figure 6. Output voltage of DC/DC Converter Without Filter

The DC-DC converter's output-side voltage, after passing through the filtering circuit is depicted in Figure 7. The filtering has effectively reduced the ripple content observed in Figure 6. The Figure 8 shows the current at the PCC for the proposed controller, while Figure 9 illustrates the power at the PCC for the same controller.

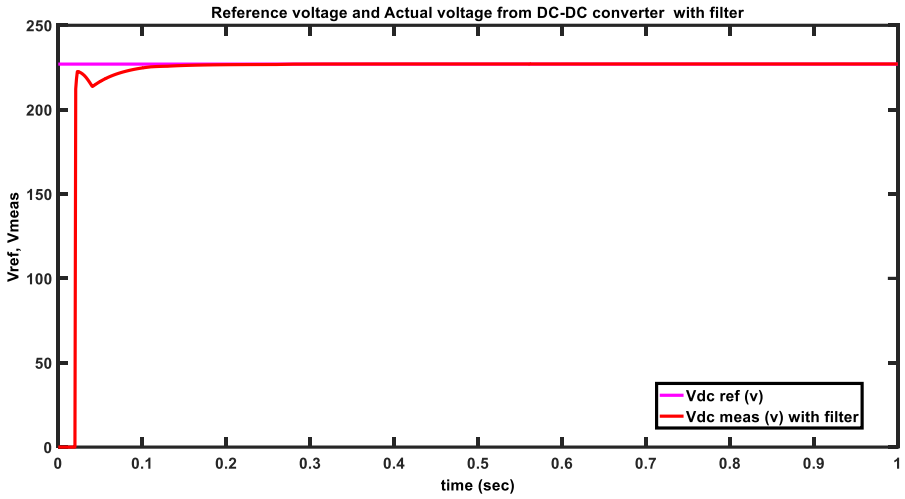

Figure 7. Voltage output of a DC/DC Converter with a Filter

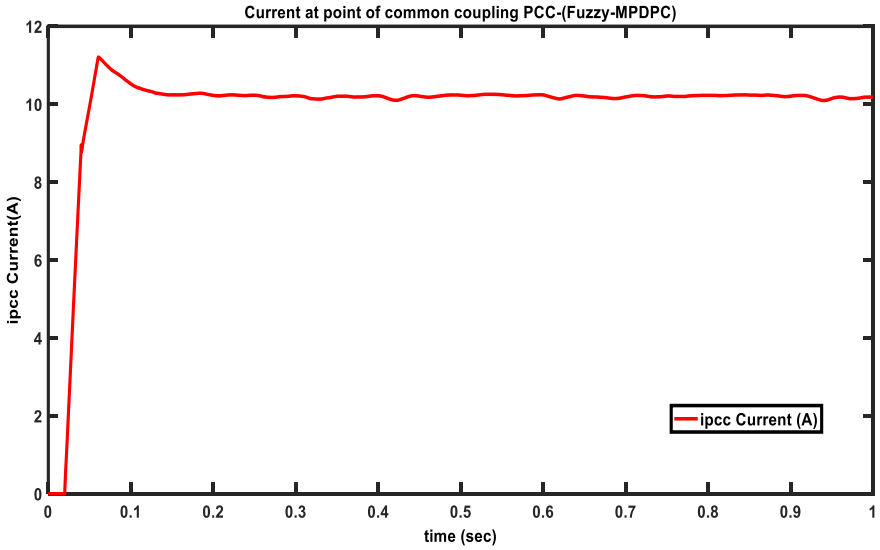

Figure 8. Current at PCC using Proposed method

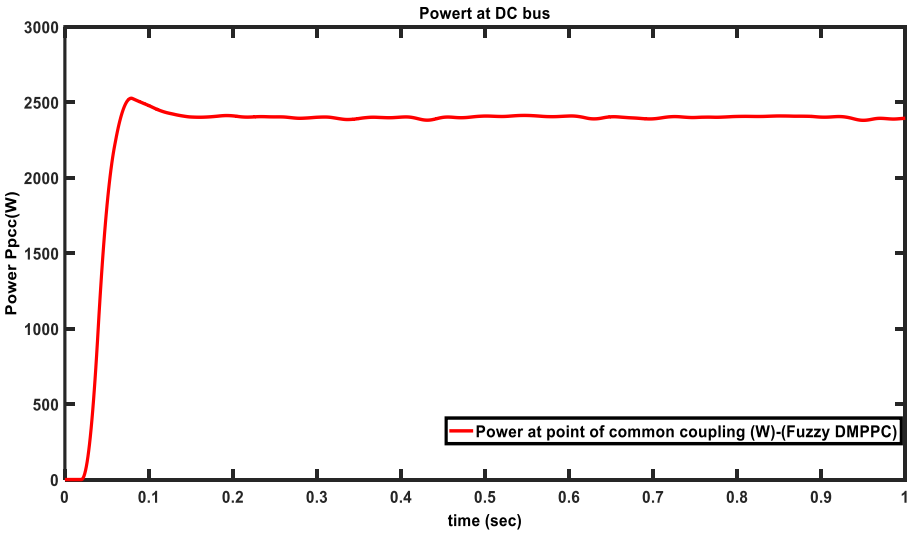

Figure 9. Power at PCC using Proposed method

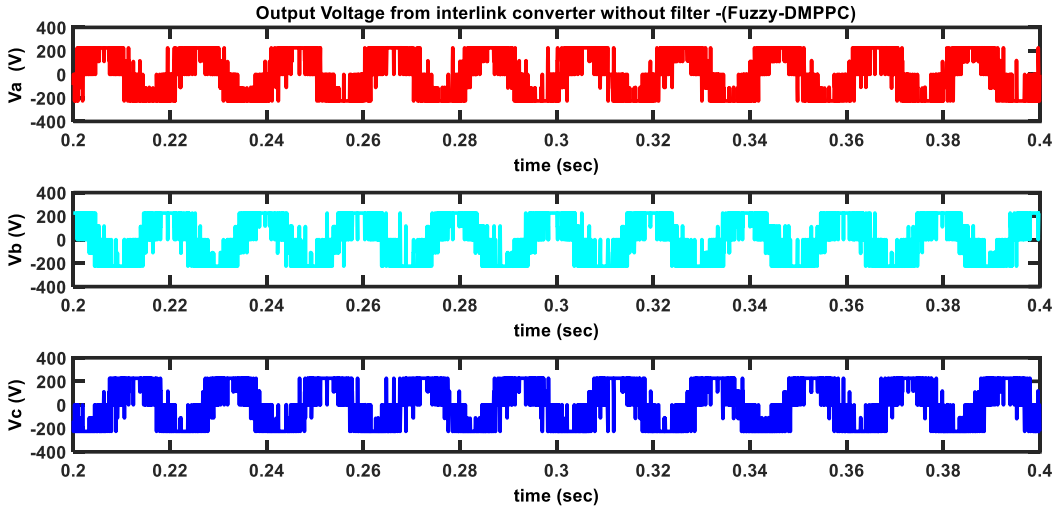

Figure 10. Interlink Converter Voltage without a Filter

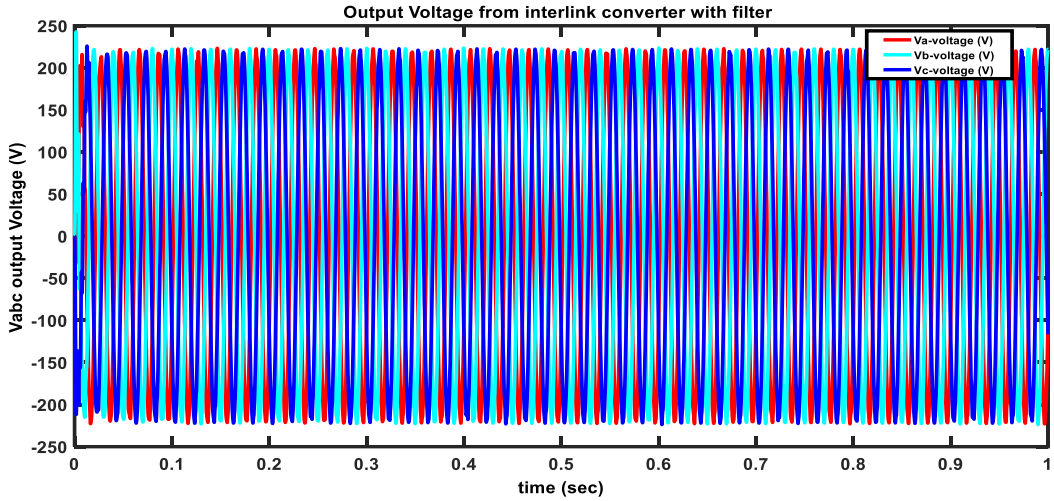

Figure 11. Interlink Converter Voltage with a Filter

In Figure 10, the leg voltages Va, Vb, and Vc of the interlink converter are displayed. The voltage that results across the suggested interlink converter is shown in figures 10 and 11, respectively, without and with filters. Figure 11 makes it abundantly evident that the converter's filter design greatly reduces ripple.

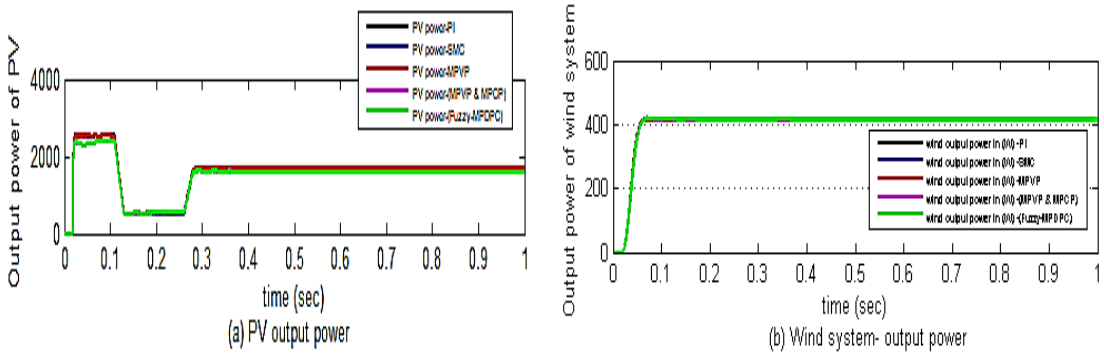

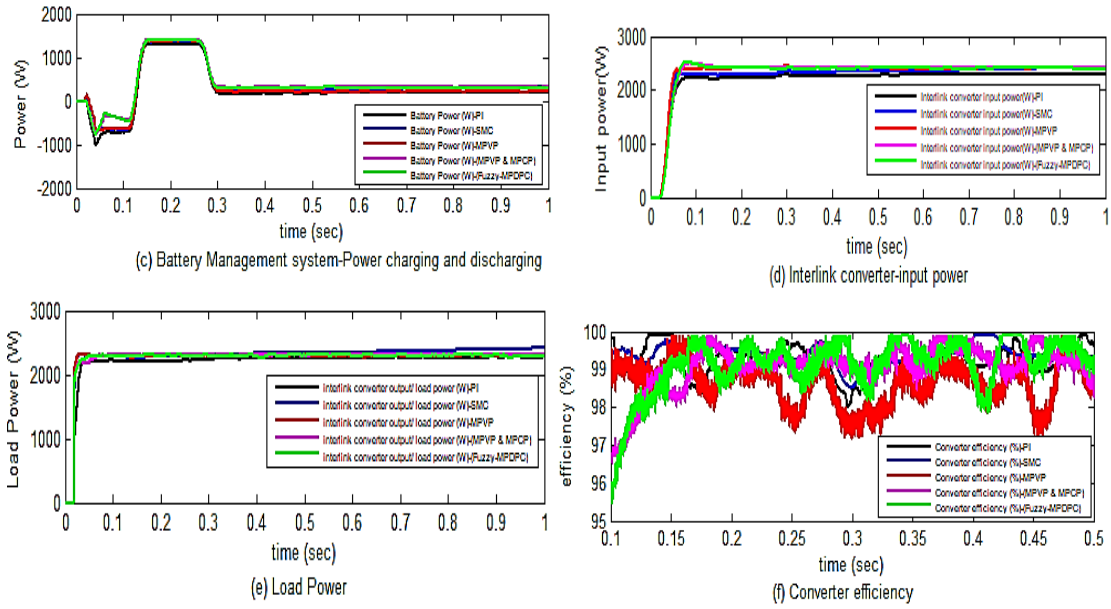

Figure 12. Various powers for different controllers for the proposed system

The power profile of the entire system under consideration is illustrated in the figure 12 for all the type of the controllers considered in this research. The power profile of PV system, Wind system, Battery Management system, converter circuit, load side and the overall efficiency of the system are all illustrated in the figure 12. From the analysis, the proposed Fuzzy-DMPPC controller's effectiveness is evident.

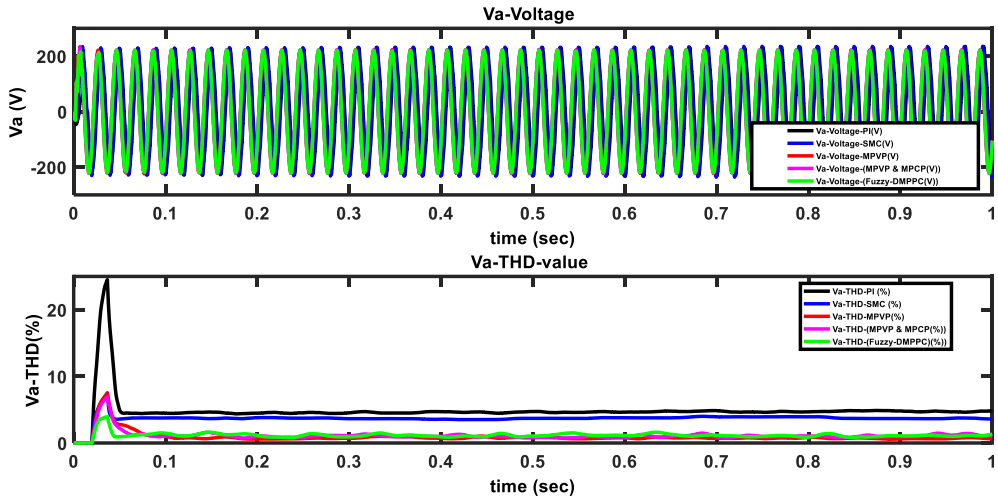

Figure 13. Comparison of the THD Value of Voltage for Each Type of Controller

Figure 13 compares the voltage output and the associated THD values for each of the all types of controllers that are taken into consideration in this paper. It is evident that when compared to the other two types taken into consideration here, the suggested Fuzzy-MPPDC control logic performs better and has a lower THD.

The input voltage to the system is given using PV panels of rating 250 W and is maintained constant as per the specifications mentioned in Table 2. Figures 14 and 15 display the system voltage and current waveforms for the suggested system in grid-connected mode and without grid-connected mode.

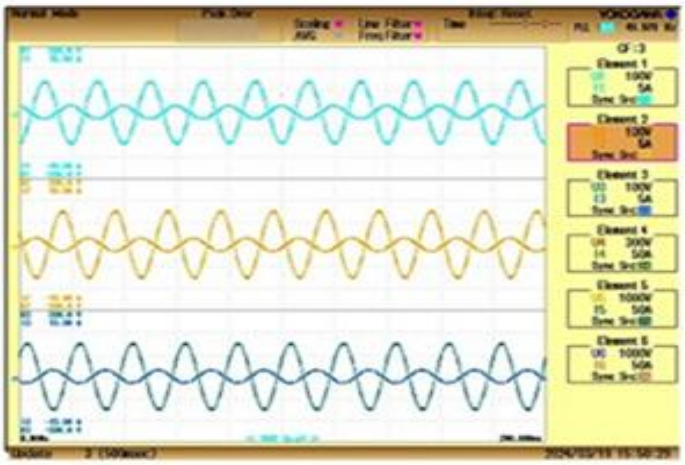

Figure 14. Waveforms of the voltage and current in the system without a grid connection

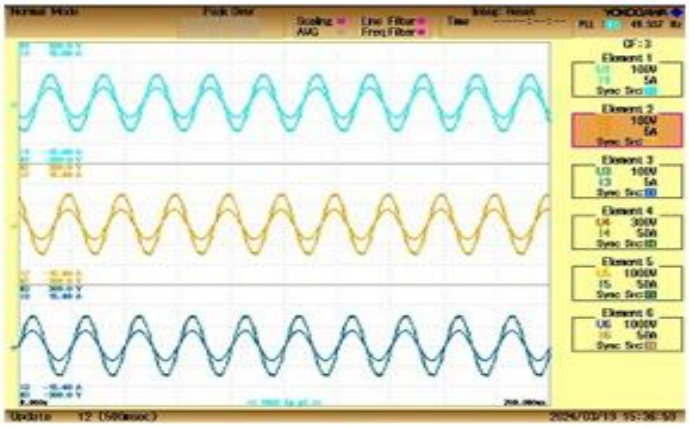

Figure 15. Waveforms of the voltage and current in the system with Grid Connected Mode

Output waveforms are captured and Total Harmonic Distortion (THD) is assessed using YOKOGAWA WT1806E power quality analyser with THD value of 0.94 % is shown in figure 16.

Figure 16. Total Harmonic Distortion of Grid Current under Grid Connected Mode

Tables 3, 4, and 5 summarize the simulation results. Table 4 specifically presents the Total Harmonic Distortion percentages at voltage output and currents under various controller types, both with and without filters. Tables 5 and 6 provide a summary of the converter efficiency and settling time for each controller under transient conditions, respectively.

Table 3. Comparison of %THD of various controllers

ON-Loaded Condition		Fuzzy-MPPDC	MPVP & MPCP (THD %)	MPVP (THD %)	SMC (%THD)	PI (%THD)
Output Voltage	**Without filter**	48.3	50.2	67.1	31.1	33.5
	With filter	0.63	0.75	1.1	6.1	14.6
Output current	**Without filter**	2.2	2.8	7.5	3.75	8.4
	With filter	0.48	0.55	0.75	2.4	2.9

Table 4. Converter efficiency of various controllers

Converter efficiency	Fuzzy-MPPDC	MPVP & MPCP	MPVP	SMC	PI
A Neutral Point Clamped (NPC) inverter-based 3-level interlink converter.	98.9	98.6	98.1	97.5	92.1

Table 5. Settling Time of various controllers

Transient condition	Fuzzy-MPPDC	MPVP & MPCP	MPVP	SMC	PI
Transient load –settling time (sec)	0.031	0.035	0.04	0.07	0.09

The prototype model's performance is analyzed in comparison with its simulation results. The experimental setup incorporates a novel Three-phase inverter configured with a diode-clamped three-level topology controlled by a Spartan 6 FPGA. The system employs 12 FGA15N120 IGBTs with integrated anti-parallel body diodes and 6 DSEP29-12B freewheeling diodes for efficient operation.

CONCLUSION

This study introduces, designs, and validates a novel Fuzzy-DMPPC controller for a hybrid grid-connected system, utilizing a interlink converter of 3-level, verified through detailed simulation analyses. The suggested controller has the ability to incorporate experience-based knowledge into the fuzzy objectives alongside limitations of the classical DMPPC objective function. The trained models can efficiently reduce the computational cost of real-time control because they are built using simple arithmetic operations unrelated to the MPC algorithm's complexityThe proposed controller consistently outperforms all other controllers evaluated in this study across various performance metrics. The voltage's THD values for the suggested logic are 0.63%, which is lowest as compared with the other types. In prototype model under grid connected mode, the THD value is 0.94% comparatively less with simulation value of various converters. Additionally, the converter efficiency has significantly increased to 98.9% as related to the other controllers. Table 5 indicates that there has also been an improvement in the settling time as well. In light of this, it can be said that the proposed The Fuzzy-DMPPC system efficiently regulates the AC/DC interlinking converter, maintaining a stable AC supply and optimal power transfer among the microgrid and the utility power grid.

Conflict of Interest

The authors certify no conflict of interest.

REFERENCES

[1] Moghadasi A, Sargolzaei A, Anzalchi A, Moghaddami M, Khalilnejad A, Sarwat A. A model predictive power control approach for a three-phase single-stage grid-tied PV module-integrated converter. IEEE Transactions on Industry Applications. 2017 Dec 27;54(2):1823-31. https://doi.org/10.1109/TIA.2017.2787626

[2] Mohankumar M, Balamurugan K, Singaravel G, Menaka SR. A Dynamic Workflow Scheduling Method based on MCDM Optimization that Manages Priority Tasks for Fault Tolerance. International Academic Journal of Science and Engineering. 2024;11(1):09-14. https://doi.org/10.71086/IAJSE/V11I1/IAJSE1102

[3] Dong H, Xu Z, Song P, Tang G, Xu Q, Sun L. Optimized power redistribution of offshore wind farms integrated VSC-MTDC transmissions after onshore converter outage. IEEE Transactions on Industrial Electronics. 2016 Nov 21;64(11):8948-58. https://doi.org/10.1109/TIE.2016.2631136

[4] Dinesh R, Myilraj R, Ragul G, Kumar TR, Singaravel G. Energy Efficient Task Allocation Algorithm for Fog Computing Networks. International Journal of Advances in Engineering and Emerging Technology. 2023 Apr 30;14(1):46-51.

[5] Han Y, Li H, Shen P, Coelho EA, Guerrero JM. Review of active and reactive power sharing strategies in hierarchical controlled microgrids. IEEE Transactions on Power Electronics. 2016 May 25;32(3):2427-51. https://doi.org/10.1109/TPEL.2016.2569597

[6] Ikechukwu O, Ikpe Aniekan E, Paul S. Design of a Beam Structure for Failure Prevention at Critical Loading Conditions. International Academic Journal of Innovative Research. 2019;6(1):53-65. https://doi.org/10.9756/IAJIR/V6I1/1910005

[7] Shadmand MB, Li X, Balog RS, Abu Rub H. Constrained decoupled power predictive controller for a single-phase grid-tied inverter. IET Renewable Power Generation. 2017 Apr;11(5):659-68. https://doi.org/10.1049/iet-rpg.2016.0520

[8] Boopathy EV, Niranjana MI, Prasath S, Sivabalvigneshan P, Sanjesh R, Sanjay S, Nithishkumar A, Vishal S. Aegis Flare: IOT-Enabled Robotic Firefighter for Advanced Fire Detection and Suppression. Archives for Technical Sciences/Arhiv za Tehnicke Nauke. 2025 Jan 1(32). https://doi.org/10.70102/afts.2025.1732.066

[9] Kumar PS, Lenine D, Kiran PS, Tummala SK, Al-Jawahry HM, Singh S. Energy management system for small scale hybrid wind solar battery based microgrid. InE3S Web of Conferences 2023 (Vol. 391, p. 01138). EDP Sciences. https://doi.org/10.1051/e3sconf/202339101138

[10] Kang J, Kim J, Sohn MM. Supervised learning-based Lifetime Extension of Wireless Sensor Network Nodes. J. Internet Serv. Inf. Secur. 2019 Nov;9(4):59-67.

[11] Chaiyatham T, Ngamroo I. Improvement of power system transient stability by PV farm with fuzzy gain scheduling of PID controller. IEEE Systems Journal. 2014 Sep 4;11(3):1684-91. https://doi.org/10.1109/JSYST.2014.2347393

[12] Lee JH, Teraoka F. Guest editorial: Advances in wireless mobile and sensor technologies. Journal of Wireless Mobile Networks, Ubiquitous Computing, and Dependable Applications. 2010 Sep;1(2-3):1-2.

[13] Benadli R, Bjaoui M, Khiari B, Sellami A. Sliding mode control of hybrid renewable energy system operating in grid connected and stand-alone mode. Power Electronics and Drives. 2021;6. https://doi.org/10.2478/pead-2021-0009

[14] Kayalvizhi S, Kumar DV. Load frequency control of an isolated micro grid using fuzzy adaptive model predictive control. IEEE Access. 2017 Aug 14; 5:16241-51. https://doi.org/10.1109/ACCESS.2017.2735545

[15] Liu X, Wang D, Peng Z. Cascade-free fuzzy finite-control-set model predictive control for nested neutral point-clamped converters with low switching frequency. IEEE Transactions on Control Systems Technology. 2018 Jun 26;27(5):2237-44. https://doi.org/10.1109/TCST.2018.2839091

[16] Wang B, Yang L, Wu F, Chen D. Fuzzy predictive functional control of a class of non-linear systems. IET Control Theory & Applications. 2019 Sep;13(14):2281-8. https://doi.org/10.1049/iet-cta.2018.5903

[17] Liu X, Wang D, Peng Z. Cascade-free fuzzy finite-control-set model predictive control for nested neutral point-clamped converters with low switching frequency. IEEE Transactions on Control Systems Technology. 2018 Jun 26;27(5):2237-44. https://doi.org/10.1109/TCST.2018.2839091

[18] Hu J, Xu Y, Cheng KW, Guerrero JM. A model predictive control strategy of PV-Battery microgrid under variable power generations and load conditions. Applied Energy. 2018 Jul 1; 221:195-203. https://doi.org/10.1016/j.apenergy.2018.03.085

[19] Suresh P, Lenine D. Design and Investigation of Sliding Mode Control Based DC-link Converter of Hybrid Microgrid System. International Journal of Integrated Engineering. 2024 Nov 24;16(3):346-57.

[20] Priyanka G, Kumari JS, Lenine D, Tummala SK, Al-Jawahry HM, Gupta H. Reduced Common Mode Multilevel Inverter Strategy in Photovoltaic Systems. InE3S Web of Conferences 2023 (Vol. 391, p. 01136). EDP Sciences. https://doi.org/10.1051/e3sconf/202339101136

[21] Bozorgi AM, Gholami-Khesht H, Farasat M, Mehraeen S, Monfared M. Model predictive direct power control of three-phase grid-connected converters with fuzzy-based duty cycle modulation. IEEE Transactions on Industry Applications. 2018 May 22;54(5):4875-85. https://doi.org/10.1109/TIA.2018.2839660

[22] Ma T, Cintuglu MH, Mohammed OA. Control of a hybrid AC/DC microgrid involving energy storage and pulsed loads. IEEE Transactions on industry applications. 2016 Sep 27;53(1):567-75. https://doi.org/10.1109/TIA.2016.2613981

[23] Kumar PS, Suresh P, Lenine D. Performance improvement of predictive voltage control for interlinking converters of integrated microgrid. Measurement: Sensors. 2024 Jun 1; 33:101196. https://doi.org/10.1016/j.measen.2024.101196

[24] Kumari JS, Babu CS, Lenine D, Lakshman J. Improvement of static performance of multilevel inverter for single-phase grid connected photovoltaic modules. In2009 Second International Conference on Emerging Trends in Engineering & Technology 2009 Dec 16 (pp. 691-697). IEEE. https://doi.org/10.1109/ICETET.2009.128

[25] Shan Y, Hu J, Chan KW, Fu Q, Guerrero JM. Model predictive control of bidirectional DC–DC converters and AC/DC interlinking converters—A new control method for PV-wind-battery microgrids. IEEE

Transactions on Sustainable Energy. 2018 Oct 1;10(4):1823-33. https://doi.org/10.1109/TSTE.2018.2873390

[26] Xing X, Zhang C, He J, Chen A, Zhang Z. Model predictive control for parallel three-level T-type grid-connected inverters in renewable power generations. IET Renewable Power Generation. 2017 Sep;11(11):1353-63. https://doi.org/10.1049/iet-rpg.2016.0361

[27] Dharmasena S, Choi S. Model predictive control of five-phase permanent magnet assisted synchronous reluctance motor. In2019 IEEE Applied Power Electronics Conference and Exposition (APEC) 2019 Mar 17 (pp. 1885-1890). IEEE. https://doi.org/10.1109/APEC.2019.8722267

[28] Dong H, Xu Z, Song P, Tang G, Xu Q, Sun L. Optimized power redistribution of offshore wind farms integrated VSC-MTDC transmissions after onshore converter outage. IEEE Transactions on Industrial Electronics. 2016 Nov 21;64(11):8948-58. https://doi.org/10.1109/TIE.2016.2631136

[29] Han H, Hou X, Yang J, Wu J, Su M, Guerrero JM. Review of power sharing control strategies for islanding operation of AC microgrids. IEEE Transactions on Smart Grid. 2015 Jun 10;7(1):200-15. https://doi.org/10.1109/TSG.2015.2434849

[30] Liu Z, Miao S, Wang W, Sun D. Comprehensive control scheme for an interlinking converter in a hybrid AC/DC microgrid. CSEE Journal of Power and Energy Systems. 2020 Aug 19;7(4):719-29. https://doi.org/10.17775/CSEEJPES.2020.00970

[31] Kayalvizhi S, Kumar DV. Load frequency control of an isolated micro grid using fuzzy adaptive model predictive control. IEEE Access. 2017 Aug 14; 5:16241-51. https://doi.org/10.1109/ACCESS.2017.2735545